BRAIN RESEARCH 1563 (2014) 81–90

Available online at www.sciencedirect.com

ScienceDirect

www.elsevier.com/locate/brainres

Brain Research

Research Report

Neuroprotective effects of hypothermia on synaptic actin cytoskeletal changes induced by perinatal asphyxia

Javier Muñiz[a,1], Juan Romero[a,1], Mariana Holubiec[a,1], George Barreto[b], Janneth González[b], Madeleine Saint-Martin[a], Eduardo Blanco[a,c], Juan Carlos Cavicchia[d], Rocío Castilla[a], Francisco Capani[a,e,*]

[a]Laboratorio de Citoarquitectura y Plasticidad Neuronal, Instituto de Investigaciones Cardiológicas "Prof. Dr. Alberto C. Taquini" (ININCA), UBA-CONICET, C1122AAJ, Buenos Aires, Argentina
[b]Departamento de Nutrición y Bioquímica, Facultad de Ciencias, Pontificia Universidad Javeriana, Bogotá DC, Colombia
[c]Departamento de Psicobiología y Metodología de las Ciencias del Comportamiento, Facultad de Psicología, Universidad de Málaga, Málaga, Spain
[d]Instituto de Histología y Embriología "Dr. Mario H. Burgos" (IHEM-CONICET), Facultad de Ciencias Médicas, Universidad Nacional de Cuyo, Mendoza, Argentina
[e]Departamento de Biología, Universidad Argentina John F Kennedy, Buenos Aires, Argentina

ARTICLE INFO

Article history:
Accepted 17 March 2014
Available online 28 March 2014

Keywords:
Neostriatum
Perinatal asphyxia
Neuroprotection
Hypothermia
Actin cytoskeleton

ABSTRACT

Cerebral hypoxia–ischemia damages synaptic proteins, resulting in cytoskeletal alterations, protein aggregation and neuronal death. In the previous works, we have shown neuronal and synaptic changes in rat neostriatum subjected to hypoxia that leads to ubi-protein accumulation. Recently, we also showed that, changes in F-actin organization could be related to early alterations induced by hypoxia in the Central Nervous System. However, little is known about effective treatment to diminish the damage. The main aim of this work is to study the effects of birth hypothermia on the actin cytoskeleton of neostriatal post-synaptic densities (PSD) in 60 days olds rats by immunohistochemistry, photooxidation and western blot. We used 2 different protocols of hypothermia: (a) intrahypoxic hypothermia at 15 °C and (b) post-hypoxia hypothermia at 32 °C. Consistent with previous data at 30 days, staining with phalloidin–Alexa^{488} followed by confocal microscopy analysis showed an increase of F-actin fluorescent staining in the neostriatum of hypoxic animals. Correlative photooxidation electron microscopy confirmed these observations showing an increment in the number of mushroom-shaped F-actin staining spines in neostriatal excitatory synapses in rats subjected to hypoxia. In addition, western blot revealed β-actin increase in PSDs in hypoxic animals. The optic relative density measurement showed a significant difference between controls and hypoxic animals. When hypoxia was induced under hypothermic conditions, the changes

*Corresponding author at: Laboratorio de Citoarquitectura y Plasticidad Neuronal, Instituto de Investigaciones Cardiológicas "Prof. Dr. Alberto C. Taquini" (ININCA), UBA-CONICET, Marcelo T. de Alvear 2270, C1122AAJ, Buenos Aires, Argentina. Fax: +54 11 4508 3888.
[1] These authors contributed equally to this work.
E-mail address: fcapani@fmed.uba.ar (F. Capani).

http://dx.doi.org/10.1016/j.brainres.2014.03.023
0006-8993/

observed in actin cytoskeleton were blocked. Post-hypoxic hypothermia showed similar answer but actin cytoskeleton modifications were not totally reverted as we observed at 15 °C. These data suggest that the decrease of the body temperature decreases the actin modifications in dendritic spines preventing the neuronal death.

1. Introduction

Birth hypoxia-ischemia or perinatal asphyxia (PA) is a serious complication with a high mortality and morbidity (McGuire, 2006; Van Bel and Groenendaal, 2008). Following PA, approximately 45% of newborn die and 25% have permanent neurological deficits including cerebral palsy, mental retardation and developmental delay, learning disabilities, visual and hearing problems, and different issues in the school readiness (Hill and Volpe, 1981; Amiel-Tison and Ellison, 1986; Vannucci and Perlman, 1997; Gunn, 2000; Osborne et al., 2004; Shankaran, 2009; Titomanlio et al., 2011)

Dendritic spines are small protrusions emerging from their parent dendrites, and their morphological changes are involved in synaptic plasticity (Fukazawa et al., 2003; Dent et al., 2011; Bae et al., 2012), protein translocation (Ouyang et al., 2005) and may be involved in different brain diseases including hypoxia-ischemia (Gisselsson et al., 2005, 2010; Luebke et al., 2010; Saraceno et al., 2012a). Dendritic spines are characterized for a rich actin cytoskeleton network (Fifkova and Delay, 1982; Capani et al., 2001a, 2008). These small structures are composed of different proteins belonging to several sub-families such as membrane receptors, scaffold proteins, signal transduction proteins and cytoskeletal proteins Shirao and González-Billault (2013). Actin filaments in dendritic spines consist of double helix of actin protomers decorated with Arp 2/3 and ADF/cofilin, and the balance between them is closely related to actin dynamic, which may govern morphological and functional synaptic plasticity (Fukazawa et al., 2003; Pollard and Borisy, 2003; Cingolani et al., 2008; Shirao and González-Billault, 2013). Different kinds of dendritic spines were described based on its shape and their content of actin in adult rat brain. Mushroom-shaped spines have stalks with a clear heads differentiation, stubby spines are thick and have no neck and thin spines are characterized for being long and without neck (Capani et al., 2001c).

For decades, neuroprotective options have been explored, however, at the moment there are currently no effective therapies. Hypothermia has outcome as an important tool to reduce the damage after experimental brain ischemia (Capani et al., 1997, 2001b, 2003; Clark et al., 2009; Sameshima and Ikenoue; 2013). In addition, hypothermia has shown good results although focused only on the therapy for neonatal encephalopathy (Shankaran, 2009; Sameshima and Ikenoue; 2013; Wu and Grotta, 2013).

In previous works, we have observed long term alterations in dendritic spines, high level of ubiquitinization, increment in astrocytes reactivity and alterations in dendritic microtubular organization after PA (Capani et al., 2009; Saraceno et al., 2010; Saraceno et al., 2012b). In addition, recently we have described early modifications in the neostriatum synaptic actin cytoskeleton. In this report we aimed to investigate whether hypothermia can prevent alterations in the actin cytoskeleton of dendritic spines after 60 days of induction of PA using correlative light and electron microscopy for phalloidin–eosin and western blot analysis. We used to different protocols of hypothermia: (a) intrahypoxic hypothermia, since we have obtained in the last years clear evidence of its efficiency to totally block hypoxic damage, and (b) post hypoxia hypothermia at 32 °C.

2. Results

2.1. *Effect of temperature on neostriatal cell survival in vivo*

Staining of neostriatal sections with cresyl violet revealed clear nuclear condensation after 2 months in rats subjected to 20 min of PA (Fig. 1A). Slight nuclear condensation was also observed after 10 and 15 min of PA (Fig. 1A). To determine the nature of the condensed cells, a conventional electron microscopy study was performed. We observed that most cells showing nuclear condensation have morphological characteristics corresponding to neurons in degeneration, such as dark cytoplasm with vacuoles, nucleus compaction, a nucleus with a festoon shape and twisted nuclear envelope (Capani et al., 1997, 2009; Aggoun-Zouaoui et al., 1998; Liu et al., 2004). In contrast, these ultrastructural alterations were not observed in neither using both protocol of hypothermic or control groups (Fig. 2B).

2.2. *Analysis of striatal GABAergic neuronal loss*

To quantify the loss of neurons in neostriatum we employed stereology combined with calbindin immunostaining, which identifies GABAergic neurons in neostriatum (Van den Berg et al., 2003; Capani et al., 2009). We focused only on GABAergic neurons since they represent the target of glutamate synapses from the cortex. Statistics indicated lower means of calbindin IR neurons as compared to the control group, the longer the exposure time of PA was. The overall ANOVA was significant ($P < 0.05$) and post hoc tests showed that the decrement of the means of calbindin IR neurons was statistically significant only at 20 min of PA ($P < 0.05$) while the mean of the HYP 20 min and HYP 20 min 32 °C group were not significantly different from the control group (see Table 1).

2.3. *F-actin staining in neostriatum dendritic spines*

Punctuate staining, representative of areas rich in dendritic spines, was observed at confocal level using phalloidin–Alexa^{488}. Increase in punctuate staining was observed after 20 min of PA,

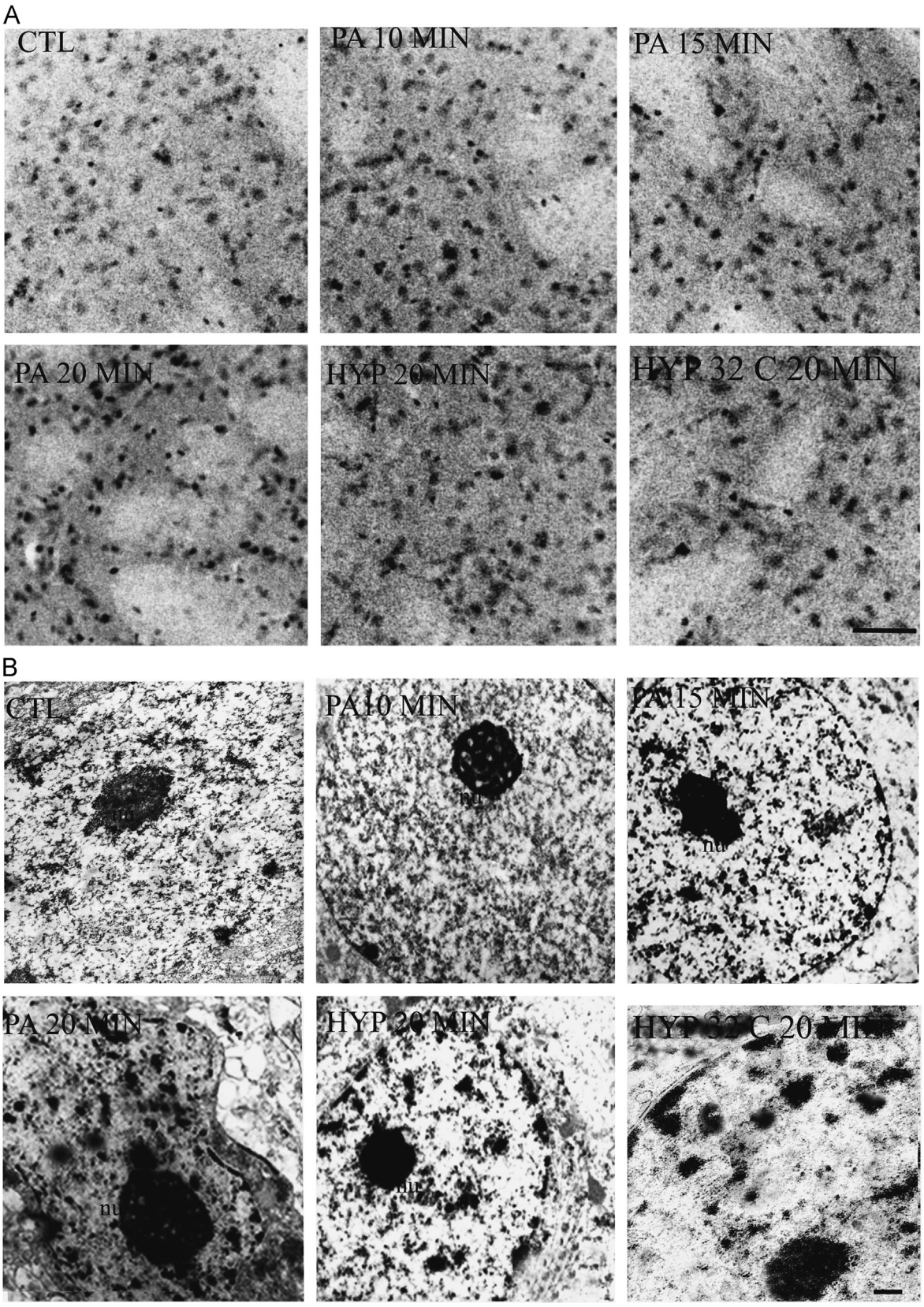

Fig. 1 – Top: low-power micrographs neostriatum from 60 days old CTL rats and animals subjected to different times of PA. Neostriatal sections were stained with cresyl violet. A clear nuclear condensation was observed after 20 min of PA (arrows). In both protocols of hypothermia nucleus appeared with the same characteristic than the control. Scale bar, 30 μm. Bottom: ultrastructural organization of the GABAergic neurons in the neostriatum area from two months old CTL rats and animals subjected to different time of PA. Note that the morphological characteristics of neurodegeneration in the 20 min PA rats are pronounced. Tissue subjected to both protocols of hypothermia showed the similar preservation that the control neurons. Nu, nucleus. Scale bar: 1 μm.

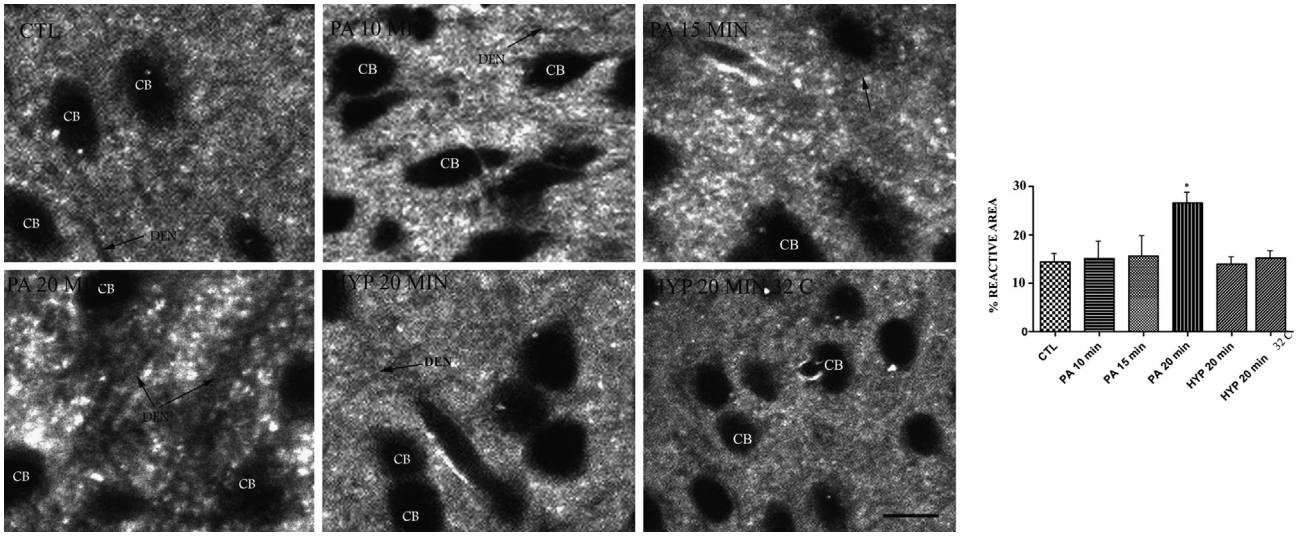

Fig. 2 – Confocal microscope images of phalloidin–Alexa488 from neostriatum area from two month old control, asphyctic and rats subjected to hypothermia rats. An increase in the punctate staining was observed after 20 min of PA (arrows). In both protocols of hypothermia showed the same pattern of distribution of the punctate than the control. The assessment of the percentage of the reactive area from striatal phalloidin–Alexa488 staining in PA rats showed an increment in the reactivity area staining with phalloidin. *$P<0.01$. Bars and error bars represent mean 1 SEM. DEN, dendrites; CB, cell body. Scale bar: 10 μm.

Table 1 – Estimates of the mean total number of calbindin-immunoreactive neurons in the neostriatum.

Groups	Means	Calbindin IR neurons	% cell loss
Control	613.32	87.29	
PA 10 min	532.12	83.29	−11.0
PA 15 min	527.13	109.5	−12.0
PA 20 min	432.23	104.6*	−25.3
HYP 20 min 15 °C	603.02	83.6	−1.1
HYP 20 min 32 °C	572.02	74	−5.7

Data are expressed as means ± SD. Each experimental group was compared to the control group (see text for statistical details).
* $P<0.05$.

while 10 and 15 min of asphyxia showed a pattern of staining similar to the control group. Moreover, hypothermia dramatically reduced the pattern of phalloidin-labelling (Fig. 2).

The morphometric analysis confirmed these data. Dendritic spines of animals subjected to 20 min of PA showed a significant increment in the reactive area stained with phalloidin ($P<0.001$) in comparison with control. Since mushroom type dendritic spines are a structure with highly concentrated F-actin (Capani et al., 2001c), we may infer that the increment observed in F-actin is a consequence of an increment in the number of these dendritic spines. On the other hand, hypothermia treatment using both protocols dramatically blocked the increase in F-actin, as showing the by the reactive area of phalloidin staining comparable to control animals (Fig. 3)

2.4. *Correlative photooxidation with phalloidin–eosin*

Among others, our group has used correlative light and electron microscopy with phalloidin–eosin in several different studies (Capani et al., 2001a, c, 2008; Fukazawa et al., 2003; Ouyang et al., 2005) which is a consistent technique to study actin changes in different populations of dendritic spines. Analyses of spines population in the photoxidated samples at electron microscopic level confirm confocal microscope observations. An increment in the number of F-actin positive spines was observed after 20 min of PA. No changes in the number of phalloidin-positive dendritic spines in animals suffering 10 and 15 min of PA (Fig. 3). When we analyzed the different populations of dendritic spines we observed that only the mushroom spines, the only ones positive for F-actin, significantly increased in number after 20 min of PA ($P<0.001$). Synapses showed no signs of evident degeneration in rats treated with asphyxia and hypothermia for different times. On the other hand, animals treated with hypothermia halted the overexpression of actin filaments in the neostriatal spines-mushrooms type (Fig. 3)

2.5. *Western blot analysis of PSD fraction*

The β actin expression in isolated PSD fractions was analyzed by immunoblotting using anti-β actin antibody and quantified (Fig. 4). Statistical analysis indicated significant differences between the mean optical densities ($P<0.01$). Post hoc tests indicated that β actin expression at 20 min PA was significantly higher in comparison with the control group or others asphyctic groups ($P<0.01$ for all comparisons). On the contrary, the β actin expression in the HYP 20 min group was not significantly different of the control group ($P>0.05$) (Fig. 4). However, no significance difference was observed using post hypoxic hypothermia protocol, suggesting that the cool treatment was not enough to prevent molecular changes. Western blot analysis strongly supported the observations at light and electron microscopic levels.

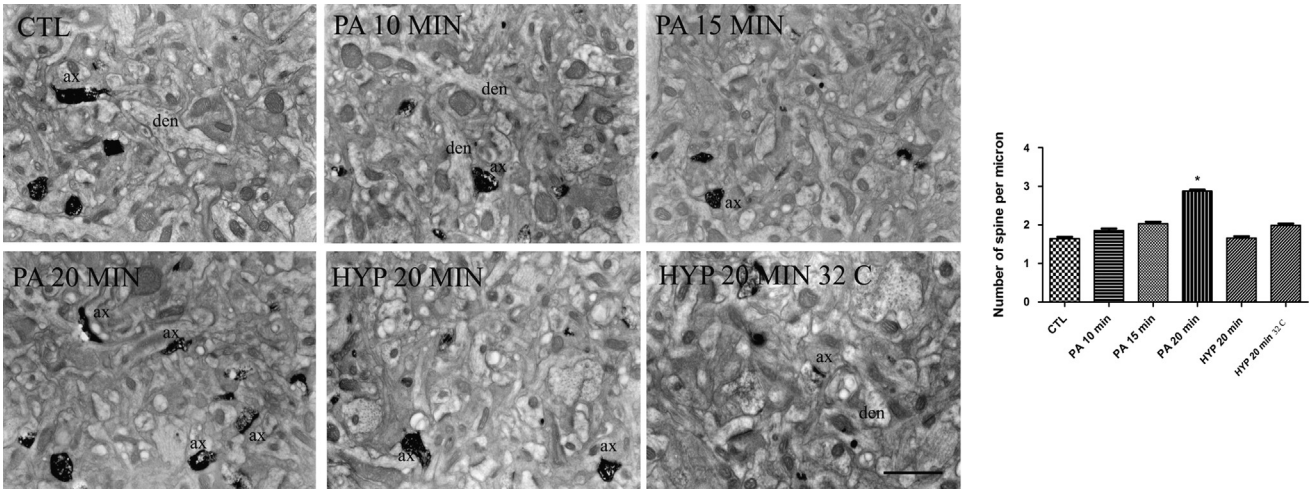

Fig. 3 – Electron micrograph of photooxidated area in the neostriatum of 2 month old rat from the different experimental conditions. Arrows point out the dendritic spines stained. An increment in the number of the F-actin positive spines was observed after 20 min of PA. Hypothermia treated rats preserved the dendritic spines actin cytoskeleton. AT, Axon terminal; DEN, dendritic shaft. Scale bar: 1 μm. The graph shows the assessment of the number of spines per field from striatal slices. A significant increment in the number of positive F-actin spines was observed in the PA group in comparison with the CTL group. *$P<0.01$. Bars and error bars represent mean 1 SEM.

3. Discussion

In this study, we demonstrated the hypothermia decreases the neuronal death and diminished the changes in the actin cytoskeleton in rat neostriatum of 60 days old rat, modifications induced by 20 min of perinatal asphyxia using correlative light and electron microscopic techniques and western blot. This body of data strongly supports the idea that synaptic alterations are one of the targets for hypothermia to reduce hypoxia damage

3.1. *Mechanism involved in actin changes after PA*

AP produce several changes at synaptic level which includes elevation of glutamate in the extracellular space (Choi, 1995) and different kind of aberrant cell signaling (Dunah et al., 1996; Endres et al., 1999; Martone et al., 1999; Liu et al., 2004, 2006; Li et al., 2007; Capani et al., 2009; Schafer et al., 2009). Consistent with previous report in hippocampal cells culture (Gisselsson et al., 2005), and with our data in neostriatum after 30 days of AP (Saraceno et al., 2012a) we have observed in vivo an increment in the actin staining in dendritic spines, after 1 month of asphyctic insult. We used a correlative light and electron microscopic technique that has been used for our laboratory (Capani et al., 2001a) and other (Fukazawa et al., 2003; Ouyang et al., 2005) to show that the increment in actin staining at light confocal level corresponds with the increment in mushrooms type dendritic spines actin positive, suggesting that actin could be related neuronal damage produced by hypoxia. Western blot analysis also confirmed these observations. Consistent with this point of view, treatment with cytochalasin D (a potent inhibitor of actin polymerization.) decreases the infarct size following media cerebral artery occlusion (Laufs et al., 2000). Actin cytoskeleton is highly regulated by different actin binding proteins (Pollard and Borisy, 2003). Several actin proteins have been also involved in the process of cell death during ischemia. Disruption of receptor-scaffold protein as NMDA-PSD 95 that is depending of actin polymerization interactions can prevent cell death after ischemia (Aarts et al., 2002). Changes in spines morphology are strongly linked to some actin-binding proteins such as gelsolin. Gelsolin-null neurons have enhanced cell death and rapid sustained elevation of Ca^{2+} levels following glucose/oxygen deprivation, as well as augmented cytosolic Ca^{2+} levels in nerve terminals following depolarization in vitro (Endres et al., 1999). Also, gelsolin diminishes the infarct size after ischemia preventing neuronal death (Harms et al., 2004). In addition, an increment in histone acetylation induces an up-regulation of gelsolin reducing dramatically the actin filaments levels and cell death following cerebral ischemia in mice (Yildirim et al., 2008). Consistent with this data Gisselsson et al. (2010) have shown that Rho kinase inhibition, in organotypic hippocampal slices subjected to ischemia, reduces the cell death suggesting that actin depolimerization reduces cell death.

F-actin is selectively concentrated in mushroom type spines (Capani et al., 2001c). The mushrooms shape dendritic spines have been involved in protein translocation in potentiated spines in hippocampal slices (Ouyang et al., 2005), and is highly regulated by phosphorylation/desphosphorylation of cofilin, another actin-binding protein. Furthermore, Fukazawa et al. (2003) have shown that LTP induction is associated with actin cytoskeletal reorganization characterized by a long-lasting increase in F-actin content within dendritic spines. This increase in F-actin content is dependent on NMDA receptor activation and involves the inactivation of actin depolymerizing factor/cofilin. Thus, changes in the mushroom spines cytoskeleton after ischemia could be involved in different long term diseases that PA might induce.

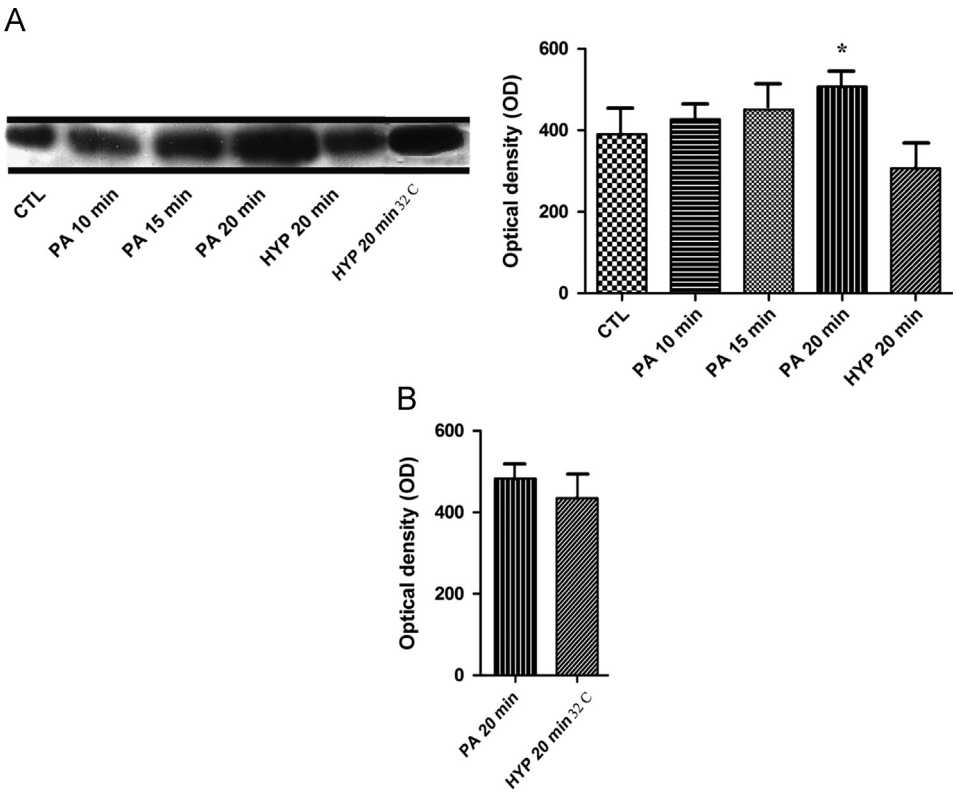

Fig. 4 – Immunoblots of striatal PSDs of one-month-old CTL and PA rats. The molecular size is indicated at the left. β-Actin is increased after 20 min of PA. (A) Intrahypoxic hypothermia rats showed the same level of expression than the control. (B) No differences in actin expression were observed between post-hypoxia hypothermia and PA. The assessment of the percentage of optical density of PSD immunoblot bands from the one-month-old CTL and PA rats showed a significant increment in the optical density respect to control group (CTL). *P < 0.01. Bars and error bars represent mean 1 SEM.

Taken together this data suggests that an early alteration in the actin cytoskeleton regulation could build an aberrant biochemical pathway that induced long term modifications in the brain of the perinatal asphyctic animals.

3.2. *Hypothermia neuroprotection and cell death*

In agreement with previous reports, hypothermia regulates the mechanisms of actin polymerization and depolymerization (Gisselsson et al., 2005). The neuroprotective effect of hypothermia has been well establish for us and others (Capani et al., 1997; Gisselsson et al., 2005, 2010). Hypothermia effect on actin cytoskeleton may alter the NMDA receptor interactions with PSD95 diminishing Ca^{++} and then reducing the cell death (Aarts et al., 2002). In addition, we (Capani et al., 2009) and Liu et al. (2006) have demonstrated that hypothermia blocked the increase of ubiquitin induced by ischemia. Some functional data showed that hypothermia significantly decreased attention deficits in the choice reaction time task and spatial learning deficits in the water maze task (Sameshima and Ikenoue; 2013). Hence, hypothermia appears to prevent the alterations of actin cytoskeleton, regulating the polymerization–depolymeration cycle and then reducing the behavioral alterations.

On other hand, we observed that intrahypoxic hypothermia has a best answer against the cytoskeletal modifications that we observed with post-hypoxia hypothermia, probably because the intrahypoxic hypothermia is induced at lower temperature than post-hypoxia hypothermia Although all of these data is experimental, it is well know that post-hypoxic hypothermia is promising useful only for severe infants encephalopathy induced by perinatal asphyxia (Soll, 2013). Therefore, we conclude that new experimental hypothermia procedure should be tested for refine our understanding of this kind of intervention.

4. Experimental procedures

4.1. *Materials*

Eosin–phalloidin and Alexa–phalloidin^{488} were purchased from Invitrogen, (Carlsbad, CA). Primary antibody anti β-actin and anti-calbindin-D28 were from Sigma Chemical Co. (St. Louis, MO, USA) Secondary antibodies against mouse were obtained from Jackson ImmunoResearch Laboratories (West Grove, PA). Paraformaldehyde, EM grade glutaraldehyde, sodium cacodylate and Durcopan ACM resin were obtained from Electron Microscopy Sciences (Fort Washington, PA); special welled tissue culture plates were obtained from MatTek (Ashland, MA).

4.2. *Animals*

All procedures involving animals were approved by the Institutional Animal Care and Use Committee at the University of

Buenos Aires (School of Medicine) and conducted according to the principles of the Guide for the Care and Use of Laboratory Animals (NIH Publications No. 80-23, revised 1996). Sprague–Dawley female rats maintained on a 12:12 h light/dark cycle in a controlled temperature (21±2 °C) and humidity (65±5%) environment were placed in individual cages at the 15th day of pregnancy. The animals had access to food (Purina chow) and tap water ad libitum. One group of animals ($n=10$) were used as surrogate mothers, another group ($n=12$) were assigned to PA procedures.

4.3. *Induction of asphyxia*

Twelve full-term pregnant rats on gestational day 22, were anesthetized (Dorfman et al., 2006), rapidly decapitated and the uterus horns were isolated through an abdominal incision and placed in a water bath at 37 °C for 10 min (6 uterus horn from 3 dams), 15 min (6 uterus horn from 3 dams) and 20 min (6 uterus horn from 3 dams) (Bjelke et al., 1991; Van den Berg et al., 2003; Capani et al., 2009). Following the same procedure, other dams ($n=3$) were hysterectomized and their uterus horns were placed in a bath at 15 °C for 20 min (hypothermia during insult group [HYP 20 min]). In this hypothermia procedure, the temperature of the pups is expected to be higher than the one set for the water bath (Engidawork et al., 2001). In addition, we and others have obtained 100% survival rate with important protective effect using the same protocol (Capani et al., 1997; Loidl et al., 1997, 2000). In the post-hypoxia hypothermia procedure, Immediately after PA, animals were placed on a clean plastic pad filled with crushed ice (fine structure) and cooled (whole body) from 37.5 °C to 32.0 °C (monitoring rectal temperature) under 1.0% halothane anesthesia (for more details see Westergren et al., 2000). When desired temperature of 32.0 °C was reached, animals were removed from the cooling pad, placed on heating pad (set to 37.0 °C) to allow slow whole body re-warming. The body temperature decreased about 1° during additional 20 min, but afterward, the body temperature of animals returned to normothermia, by increase of 2 °C/h (37.0 °C after approximately 3 h).

Following asphyxia, the uterus horns were rapidly opened, the pups were removed, the amniotic fluid was cleaned and the pups were stimulated to breathe by performing tactile intermittent stimulation with pieces of medical wipes for a few minutes until regular breathing was established. The umbilical cord was ligated and the animals were left to recover for 1 h under a heating lamp. When their physiological conditions improved, they were given to surrogate mothers who had delivered normally within the last 24 h. The different groups of pups were marked and mixed with the surrogate mothers' normal litters (control animals that were left undisturbed). We maintained litters of 10 pups with each surrogate mother.

4.4. *Post-asphyctic procedure*

Adult males of two month old of age (4 per group) were used. Briefly, an intracardiac perfusion was performed with normal rat Ringer's at 35 °C followed by fixative under deep anesthesia (containing 50 mg/kg ketamine, 1 mg/kg rhompun and 5 mg/kg acetopromazine in sterile saline). For light microscopic analysis, rats were perfused with 4% paraformaldehyde (made fresh from paraformaldehyde) in 0.15 M cacodylate buffer, pH 7.2. The brain was removed and fixed for additional 2 h in the same solution at 4 °C. For electron microscopic studies, a fixative containing 4% formaldehyde and 0.1% glutaraldehyde was employed (Capani et al., 2009). After 2 h of post-fixation in the same fixative, the brain was removed from the skull and coronal or sagital sections were cut at a thickness of 50–80 μm with a Vibratome (Leica). Some of these sections were stained with cresyl violet according to the procedures described in Capani et al. (1997). We have used one month old rats because of the synapses are already mature at this stage (Fiala et al., 1998).

4.5. *Photooxidation*

Vibratome sections were washed with 50 mM glycine–PBS containing 0.5% cold water fish gelatin to block nonspecific binding. Following 30 min of washing, the sections were incubated on a shaker, in a solution of 0.05% of eosin–phalloidin–0.5% cold-water fish gelatin/50 mM glycine–PBS for 2 h at 4 °C. For light microscopic studies, phalloidin conjugated to Alexa^{488} was also used because of its superior fluorescent quantum yield compared to eosin. As a negative control, eosin–phalloidin was omitted.

Tissue sections stained with eosin–phalloidin were mounted on glass-welled tissue culture dishes (Mat Tek Corp) pre-treated with polyethylenimine. The slices were fixed again for 2–5 min with 2% glutaraldehyde in 0.1 M cacodylate buffer, rinsed in buffer for several minutes, and placed in 50 mM glycine and potassium cyanide in cacodylate buffer for an additional 5 min to reduce nonspecific staining.

Photooxidation was performed on the Zeiss Axiovert described above, equipped with a 75-W xenon arc light source. The samples were immersed in a solution of 2.8 mM diaminobenzidine in 0.1 M sodium cacodylate at 4 °C bubbled with pure O_2, final pH 7.4, and then irradiated under conventional epifluorescence using a xenon lamp. After 6–8 min a brownish reaction product began to appear in place of the fluorescence. The process was stopped by halting the excitation (Capani et al., 2001c)

4.6. *Electron microscopy procedure*

Following photooxidation, tissue sections were rinsed in 0.1 M sodium cacodylate several times and incubated for 30 min with 1% osmium tetroxide in 0.1 M sodium cacodylate, pH 7.2. After several washes in double-distilled H_2O, the sections were dehydrated in an ascending ethanol series, and flat embedded in Durcopan ACM resin and polymerized for 24 h at 60 °C. Serial thin sections (80–100 nm) were cut with Reichert Ultracut E ultramicrotome using glass knives and examined using a JEOL 100CX electron microscope at 80–100 keV. One set of thin sections was post-stained with a combination of uranyl acetate and lead citrate.

4.7. Morphometric analysis

The volume fraction of immunoreactive material for phalloidin was estimated using the point-counting method of Weibel (Weibel and Kiessling, 1978) and a grid delimiting 5000 μm^2 in the striatum. A total area of 75,000 μm^2 was evaluated in each animal. Percentage of reactive area was estimated using Image J Program (Image J 1.41o, NIH, USA).

For electron microscopy analysis sampling procedures were adapted from Harris et al. (1992) and Capani et al. (2001c). For analysis, spines were sampled from dorsal neostriatum. All synapses with characteristic of mushrooms type dendritic spines (head larger than the neck) were used in this study since mushrooms spines are the unique F-actin positive spines (Capani et al. 2001c). Random fields of neuropil containing at least one synapse were photographed at 10,000× magnification and analyzed at a total magnification of 30,000×. We analyzed 510 control spines and 1538 spines for tissue subjected to hypoxia and 528 dendrites spines from tissue subjected to HYP.

4.8. Stereological analysis of calbindin

Striatum was defined according to Paxinos and Watson (1986). Different lines were drawn to define the exact area to be quantified. Medially a line was drawn from the dorsal tip of the left-brain side to the top of the corpus callosum. Dorsal and lateral boundaries were defined by the corpus callosum; a line drawn from the ventral tip of the lateral ventricle to the rhinal fissure was used as a ventral boundary. Laterally a line was drawn from the ventral tip of the lateral ventricle to the corpus callosum. Anterior and posterior boundaries for the striatum were set at bregma 1.6 mm and −0.8 mm. (Hof and Schmitz, 2000; Capani et al., 2009).

For estimates of the total number of immunoreactive (IR) calbindin neurons, every 8th section of the brains of control ($n=4$), PA (10 min [$n=6$], 15 min [$n=6$], 19 min [$n=8$] and hypothermia ($n=8$) treated animals were analyzed using the optical dissector.

The CAST-Grid software (Olympus, Denmark) was used for quantification. The IR neurons, which came into focus within approximately 450 systematically randomly spaced dissectors, were counted at a final magnification of 3600× (distance between dissectors in mutually orthogonal directions x and y on the sections: 250 μm). The optical dissectors had a base area of 1250 μm^2. Estimated total numbers of IR neurons were calculated from the number of counted neurons and the sampling probability (Schmitz and Hof, 2000). Sampling was optimized for prevention of type II error probability due to stereological sampling. The precision of the estimated total numbers of neurons was predicted following the methods designed in Schmitz and Hof (2000) and Capani et al. (2009).

4.9. Subcellular fractionation and preparation of PSDs

Biochemical fractionation was performed as described previously by Dunah and Standaert (2003). Dounce homogenates (H) of the pellets in ice-cold TEVP buffer [10 mM Tris–HCl, pH 7.4, 5 mM NaF, 1 mM Na_3VO_4, 1 mM EDTA, and 1 mM EGTA, 1.25 μg/ml pepstatin A, 10 μg/ml leupeptin, 2.5 μg/ml aproptonin, 0.5 mM PMSF] containing 320 mM sucrose was centrifuged at 1000 × g to remove nuclei and large debris (P1). The supernatant (S1) was centrifuged at 10,000 × g to obtain a crude synaptosomal fraction (P2) and subsequently was lysed hypo-osmotically and centrifuged at 25,000 × g to pellet a synaptosomal membrane fraction (LP1). After each centrifugation the resulting pellet was rinsed briefly with ice-cold TEVP buffer before subsequent fractionations to avoid possible crossover contamination. Protein was quantified by Bradford's method (Bradford 1976) [12] using bovine serum albumin as standard.

4.10. Western blot

Western blot analysis was carried out using PSD fractions separated on 10% SDS-PAGE and the transfer of separated proteins to polyvinylidene difluoride (PVDF) membrane were performed as described previously (Wang et al., 1995; Dunah et al., 1996; Luo et al., 1996). Samples containing 20 μg of protein from each groups were applied to each lane. After electrophoresis, proteins were transferred to an Immobilon-P membrane (Amersham). The membranes were incubated with a primary antibody anti β-actin (Sigma, 1:1000) overnight at 4 °C. The membranes were incubated with horseradish peroxidase-conjugated anti-mouse secondary antibody for 2 h at room temperature. The blots were developed with an ECL detection kit (Amersham). The films were scanned, and the optical density of protein bands was quantified using Gel Pro Analizer software 3.1.00.00 (Media Cybernetics, USA). We used the Ponceau Red (Sigma, USA) staining like load control because the LP1 fraction that we use has the deficient that all of the proteins involved in these structures are affected by PA.

4.11. Statistical analysis

Material from four rats was analyzed for each experimental group and for each parameter studied. Data are expressed as mean ± SEM. Then for statistical analysis was the number of animals ($n=4$ in each experimental group). Multiple statistical comparisons were carried out with a one-way analysis of variance. Bonferroni's test was used for post hoc comparisons of mean values. A level of significance of $P<0.05$ was selected.

Acknowledgments

This research has been supported by a grant to FC from the CONICET (PIP 2011–2013, #11420100100135) and the Universidad de Buenos Aires (UBACyT 20–2012, #20020090100118).

REFERENCES

Aarts, M., Liu, Y., Liu, L., Besshoh, S., Arundine, M., Gurd, J.W., Wang, Y.T., Salter, M.W., Tymianski, M., 2002. Treatment of ischemic brain damage by perturbing NMDA receptor–PSD-95 protein interactions. Science. 298, 846–850.

Amiel-Tison, C., Ellison, P., 1986. Birth asphyxia in the fullterm newborn: early assessment and outcome. Dev. Med. Child Neurol. 28, 671–682.

Aggoun-Zouaoui, D., Margalli, I., Borrega, F., Represa, A., Plotkine, M., Ben-Ari, Y., Charriaut-Marlangue, C., 1998. Ultrastructural morphology of neuronal death following reversible focal ischemia in the rat. Apoptosis 3, 133–141.

Bae, J., Sung, B.H., Cho, I.H., Song, W.K., 2012. F-actin-dependent regulation of NESH dynamics in rat hippocampal neurons. PLoS One. 7 (4), e34514.

Bradford, M., 1976. A rapid and sensitive method for the quantitation of microgram quantities of protein utilizing the principle of protein–dye binding. Anal. Biochem. 72, 248–254.

Bjelke, B., Andersson, K., Ogren, S.O., Bolme, P., 1991. Asphyctic lesion: proliferation of tyrosine hydroxylase-immunoreactive nerve cell bodies in the rat substantia nigra and functional changes in dopamine neurotransmission. Brain Res. 543, 1–9.

Capani, F., Loidl, F., Lopez-Costa, J.J., Selvin-Testa, A., Saavedra, J.P., 1997. Ultrastructural changes in nitric oxide synthase immunoreactivity in the brain of rats subjected to perinatal asphyxia: neuroprotective effects of cold treatment. Brain Res. 775, 11–23.

Capani, F., Deerinck, T.J., Ellisman, M.H., Bushong, E., Bobik, M., Martone, M.E., 2001a. Phalloidin–eosin followed by photo-oxidation: a novel method for localizing F-actin at the light and electron microscopic levels. J. Histochem. Cytochem. 49, 1351–1361.

Capani, F., Loidl, C.F., Aguirre, F., Piehl, L., Facorro, G., Hager, A., De Paoli, T., Farach, H., Pecci-Saavedra, J., 2001b. Changes in reactive oxygen species (ROS) production in rat brain during global perinatal asphyxia: an ESR study. Brain Res. 914, 204–207.

Capani, F., Martone, M.E., Deerinck, T.J., Ellisman, M.H., 2001c. Selective localization of high concentrations of F-actin in subpopulations of dendritic spines in rat central nervous system: a three-dimensional electron microscopic study. J. Comp. Neurol. 435, 156–170.

Capani, F., Loidl, C.F., Piehl, L.L., Facorro, G., De Paoli, T., Hager, A., 2003. Long term production of reactive oxygen species during perinatal asphyxia in the rat central nervous system: effects of hypothermia. Int. J. Neurosci. 113, 641–654.

Capani, F., Saraceno, E., Boti, V.R., Aon-Bertolino, L., Fernández, J.C., Gato, F., Kruse, M.S., Giraldez, L., Ellisman, M.H., Coirini, H., 2008. A tridimensional view of the organization of actin filaments in the central nervous system by use of fluorescent photooxidation. Biocell 32 (1), 1–8.

Capani, F., Saraceno, G.E., Botti, V., Aon-Bertolino, L., de Oliveira, D.M., Barreto, G., Galeano, P., Giraldez-Alvarez, L.D., Coirini, H., 2009. Protein ubiquitination in postsynaptic densities after hypoxia in rat neostriatum is blocked by hypothermia. Exp. Neurol. 219, 404–413.

Cingolani, L.A., Thalhammer, A., Yu, L.M., Catalano, M., Ramos, T., Colicos, M.A., Goda, Y., 2008. Activity-dependent regulation of synaptic AMPA receptor composition and abundance by beta3 integrins. Neuron 12, 749–762.

Clark, D.L., Penner, M., Wowk, S., Orellana-Jordan, I., Colbourne, F., 2009. Treatments (12 and 48 h) with systemic and brain-selective hypothermia techniques after permanent focal cerebral ischemia in rat. Exp. Neurol. 220, 391–399.

Choi, D.W., 1995. Calcium: still center-stage in hypoxic–ischemic neuronal death. Trends Neurosci. 18, 58–60.

Dent, E.W., Merriam, E.B., Hu, X., 2011. The dynamic cytoskeleton: backbone of dendritic spine plasticity. Curr. Opin. Neurobiol. 21 (1), 175–181, http://dx.doi.org/10.1016/j.conb.2010.08.013 (Epub 2010 September 9. Review).

Dorfman, V.B., Vega, M.C., Coirini, H., 2006. Age-related changes of the GABA-B receptor in the lumbar spinal cord of male rats and penile erection. Life Sci. 78, 1529–1534.

Dunah, A.W., Yasuda, R.P., Wang, Y.H., Luo, J., Davila-Garcia, M., Gbadegesin, M., Vicini, S., Wolfe, B.B., 1996. Regional and ontogenic expression of the NMDA receptor subunit NR2D protein in rat brain using a subunit-specific antibody. J. Neurochem. 67, 2335–2345.

Dunah, A.W., Standaert, D.G., 2003. Subcellular segregation of distinct heteromeric NMDA glutamate receptors in the striatum. J Neurochem. 85, 935–943.

Endres, M., Fink, K., Zhu, J., Stagliano, N.E., Bondada, V., Geddes, J.W., Azuma, T., Mattson, M.P., Kwiatkowski, D.J., Moskowitz, M.A., 1999. Neuroprotective effects of gelsolin during murine stroke. J. Clin. Invest. 103, 347–354.

Engidawork, E., Loidl, F., Chen, Y., Kohlhauser, C., Stoeckler, S., Dell'Anna, E., Lubec, B., Lubec, G., Goiny, M., Gross, J., Andersson, K., Herrera-Marschitz, M., 2001. Comparison between hypothermia and glutamate antagonism treatments on the immediate outcome of perinatal asphyxia. Exp. Brain Res. 138, 375–383.

Fiala, J.C., Feinberg, M., Popov, V., Harris, K.M., 1998. Synaptogenesis via dendritic filopodia in developing hippocampal area CA1. J. Neurosci. 18, 8900–8911.

Fifkova, E., Delay, R.J., 1982. Cytoplasmic actin in neuronal processes as a possible mediator of synaptic plasticity. J. Cell Biol. 95, 345–350.

Fukazawa, Y., Saitoh, Y., Ozawa, F., Ohta, Y., Mizuno, K., Inokuchi, K., 2003. Hippocampal LTP is accompanied by enhanced F-actin content within the dendritic spine that is essential for late LTP maintenance in vivo. Neuron 38, 447–460.

Gisselsson, L.L., Matus, A., Wieloch, T., 2005. Actin redistribution underlies the sparing effect of mild hypothermia on dendritic spine morphology after in vitro ischemia. J. Cereb. Blood Flow Metab. 25, 1346–1355.

Gisselsson, L., Toresson, H., Ruscher, K., Wieloch, T., 2010. Rho kinase inhibition protects CA1 cells in organotypic hippocampal slices during in vitro ischemia. Brain Res. 1316, 92–100.

Gunn, A.J., 2000. Cerebral hypothermia for prevention of brain injury following perinatal asphyxia. Curr. Opin. Pediatr. 12, 111–115.

Harms, C., Bosel, J., Lautenschlager, M., Harms, U., Braun, J.S., Hortnagl, H., Dirnagl, U., Kwiatkowski, D.J., Fink, K., Endres, M., 2004. Neuronal gelsolin prevents apoptosis by enhancing actin depolymerization. Mol. Cell. Neurosci. 25, 69–82.

Harris, K.M., Jensen, F.E., Tsao, B., 1992. Three-dimensional structure of dendritic spines and synapses in rat hippocampus (CA1) at postnatal day 15 and adult ages: implications for the maturation of synaptic physiology and long-term potentiation. J. Neurosci. 12, 2685–2705.

Hill, A., Volpe, J.J., 1981. Seizures, hypoxic–ischemic brain injury, and intraventricular hemorrhage in the newborn. Ann. Neurol. 10, 109–121.

Hof, P.R., Schmitz, C., 2000. Current trends in neurostereology – introduction to the special issue "Recent advances in neurostereology. J. Chem. Neuroanat. 20, 3–5.

Laufs, U., Gertz, K., Huang, P., Nickenig, G., Bohm, M., Dirnagl, U., Endres, M., 2000. Atorvastatin upregulates type III nitric oxide synthase in thrombocytes, decreases platelet activation, and protects from cerebral ischemia in normocholesterolemic mice. Stroke 31, 2442–2449.

Li, D., Shao, Z., Vanden Hoek, T.L., Brorson, J.R., 2007. Reperfusion accelerates acute neuronal death induced by simulated ischemia. Exp. Neurol. 206, 280–287.

Liu, C.L., Martone, M.E., Hu, B.R., 2004. Protein ubiquitination in postsynaptic densities after transient cerebral ischemia. J. Cereb. Blood Flow Metab. 24, 1219–1225.

Liu, J.J., Zhao, H., Sung, J.H., Sun, G.H., Steinberg, G.K., 2006. Hypothermia blocks ischemic changes in ubiquitin distribution and levels following stroke. Neuroreport 17, 1691–1695.

Loidl, C.F., Capani, F., Lopez-Costa, J.J., Selvin-Testa, A., Lopez, E.M., Goldstein, J., Pecci-Saavedra, J., 1997. Short-term changes in

NADPH-diaphorase reactivity in rat brain following perinatal asphyxia. Neuroprotective effects of cold treatment. Mol. Chem. Neuropathol. 31, 301–316.
Loidl, C.F., Gavilanes, A.W., Van Dijk, E.H., Vreuls, W., Blokland, A., Vles, J.S., Steinbusch, H.W., Blanco, C.E., 2000. Effects of hypothermia and gender on survival and behavior after perinatal asphyxia in rats. Physiol. Behav. 68, 263–269.
Luebke, J.I., Weaver, C.M., Rocher, A.B., Rodriguez, A., Crimins, J.L., Dickstein, D.L., Wearne, S.L., Hof, P.R., 2010. Dendritic vulnerability in neurodegenerative disease: insights from analyses of cortical pyramidal neurons in transgenic mouse models. Brain Struct. Funct. 214 (2-3), 181–199.
Luo, L., Chen, H., Zirkin, B.R., 1996. Are Leydig cell steroidogenic enzymes differentially regulated with aging?. J. Androl. 17, 509–515.
Martone, M.E., Jones, Y.Z., Young, S.J., Ellisman, M.H., Zivin, J.A., Hu, B.R., 1999. Modification of postsynaptic densities after transient cerebral ischemia: a quantitative and three-dimensional ultrastructural study. J. Neurosci. 19, 1988–1997.
McGuire, W., 2006. Perinatal asphyxia. Clin. Evid., 511–519.
Osborne, N.N., Casson, R.J., Wood, J.P., Chidlow, G., Graham, M., Melena, J., 2004. Retinal ischemia: mechanisms of damage and potential therapeutic strategies. Prog. Retinal Eye Res. 23, 91–147.
Ouyang, Y., Wong, M., Capani, F., Rensing, N., Lee, C.S., Liu, Q., Neusch, C., Martone, M.E., Wu, J.Y., Yamada, K., Ellisman, M.H., Choi, D.W., 2005. Transient decrease in F-actin may be necessary for translocation of proteins into dendritic spines. Eur. J. Neurosci. 22, 2995–3005.
Paxinos, G.P., Watson, C., 1986. The Rat Brain Stereotaxic Coordinates. Academic Press, Sydney.
Pollard, T.D., Borisy, G.G., 2003. Cellular motility driven by assembly and disassembly of actin filaments. Cell 112, 453–465.
Sameshima H., Ikenoue T., 2013. Hypoxic–ischemic neonatal encephalopathy: animal experiments for neuroprotective therapies. Stroke Res. Treat. 2013, 659374, http://dx.doi.org/10.1155/2013/659374 (Epub 2013 February 27).
Saraceno, G.E., Bertolino, M.L., Galeano, P., Romero, J.I., Garcia-Segura, L.M., Capani, F., 2010. Estradiol therapy in adulthood reverses glial and neuronal alterations caused by perinatal asphyxia. Exp. Neurol. 223 (2), 615–622.
Saraceno, G.E, Castilla, R., Barreto, G.E., Gonzalez, J., Kölliker-Frers, R.A., Capani, F., 2012a. Hippocampal dendritic spines modifications induced by perinatal asphyxia. Neural Plast. 2012, 873532, http://dx.doi.org/10.1155/2012/873532.
Saraceno, G.E., Ayala, M.V., Badorrey, M.S., Holubiec, M., Romero, J.I., Galeano, P., Barreto, G., Giraldez-Alvárez, L.D., Kölliker-Fres, R., Coirini, F., Capani, F., 2012b. Effects of perinatal asphyxia on rat striatal cytoskeleton. Synapse 66 (1), 9–19.
Schafer, D.P., Jha, S., Liu, F., Akella, T., McCullough, L.D., Rasband, M.N., 2009. Disruption of the axon initial segment cytoskeleton is a new mechanism for neuronal injury. J. Neurosci. 29, 13242–13254.
Schmitz, C., Hof, P.R., 2000. Recommendations for straightforward and rigorous methods of counting neurons based on a computer simulation approach. J. Chem. Neuroanat. 20, 93–114.
Shankaran, S., 2009. Neonatal encephalopathy: treatment with hypothermia. J. Neurotrauma 26, 437–443.
Shirao, T., González-Billault, C., 2013. Actin filaments and microtubules in dendritic spines. J. Neurochem. 126, 155–164.
Soll, R.F., 2013. Cooling for newborns with hypoxic ischemic encephalopathy. Neonatology 104, 260–262.
Titomanlio, L., Kavelaars, A., Dalous, J., Mani, S., El Ghouzzi, V., Heijnen, C., Baud, O., Gressens, P., 2011. Stem cell therapy for neonatal brain injury: perspectives and challenges. Ann. Neurol. 70, 698–712.
Van Bel, F., Groenendaal, F., 2008. Long-term pharmacologic neuroprotection after birth asphyxia: where do we stand? Neonatology 94, 203–210.
Van den Berg, W.D., Kwaijtaal, M., de Louw, A.J., Lissone, N.P., Schmitz, C., Faull, R.L., Blokland, A., Blanco, C.E., Steinbusch, H.W., 2003. Impact of perinatal asphyxia on the GABAergic and locomotor system. Neuroscience 117, 83–96.
Vannucci, R.C., Perlman, J.M., 1997. Interventions for perinatal hypoxic–ischemic encephalopathy. Pediatrics 100, 1004–1014.
Wang, P., Royer, M., Houtz, R.L., 1995. Affinity purification of ribulose-1,5-bisphosphate carboxylase/oxygenase large subunit epsilon N-methyltransferase. Protein Expr. Purif. 6, 528–536.
Weibel, H.P., Kiessling, J., 1978. The effect of noise trauma on speech discrimination in silence and under influence of party noise (author's transl). Arch. Otorhinolaryngol. 219, 413–414.
Westergren, H., Farooque, M., Olsson, Y., Holtz, A., 2000. Motor function changes in the rat following severe spinal cord injury. Does treatment with moderate systemic hypothermia improve functional outcome? Acta Neurochir. 142, 567–573.
Wu, T.C., Grotta, J.C., 2013. Hypothermia for acute ischaemic stroke. Lancet Neurol. 12 (3), 275–284 (Review).
Yildirim, F., Gertz, K., Kronenberg, G., Harms, C., Fink, K.B., Meisel, A., Endres, M., 2008. Inhibition of histone deacetylation protects wildtype but not gelsolin-deficient mice from ischemic brain injury. Exp. Neurol. 210, 531–542.